**XXXIII IAHS**
World Congress on Housing
Sustainability of the Housing Projects
September 27- October 1, 2005, Pretoria, South Africa

# THERMAL BEHAVIOR OF PCM CONTAINING WALLS: A TIME SERIES MODEL BASED ON COINTEGRATED PROCESSES AND CONDITIONAL HETEROSKEDASTICITY

**Mario De Grassi, Alessandro Carbonari**

Department of Architecture, Construction and Structures, Engineering Faculty
Polytechnic University of Marche, Ancona, Italy
e-mail: *m.degrassi@univpm.it* *alessandro.carbonari@univpm.it*

**Giulio Palomba**

Economics Department, Economics Faculty "Giorgio Fuà"
Polytechnic University of Marche, Ancona, Italy
e-mail: *giulio@dea.unian.it*

**Keywords:** Phase Change Materials, heat transfer, ECM models, GARCH models, Impulse Responses, indoor comfort

**Abstract**
The two main advantages deriving from the insertion of Phase Change Materials (PCM) inside the external envelopes of buildings are lowering temperature peaks in internal environments and shifting their occurrence in time. In this contribution the data collected from a three-month experimental campaign are elaborated through a time series model with conditional heteroskedasticity, for the evaluation of the positive effects deriving from the insertion of a PCM layer in standard stratifications of dry assembled lightweight walls. In this work the performances of two different PCM containing stratifications are compared with the ones of a standard dry assembled lightweight wall. The statistical model in this paper is able of interpreting the long memory effects that affect the temperature time series of the experimental walls, even if with the use of a small number of parameters.

## 1 Introduction

As of the early 1990s, valuable attempts to insert Phase Change Materials (PCM) waxes inside wallboards [1] were carried out, testing the thermal load relief provided by such a technology. The application of PCM can also be useful for internal use, because it allows the storage and discharge of considerable quantities of cooling and heating energy, dumping the air temperature swings [2]. At the "Renewable Energies Outdoor Laboratory" of the Polytechnic University of Marche, a PCM layer is inserted inside standard dry built lightweight walls, in order to test the improvement of thermal performances provided by PCM. Thanks to the use of a statistical approach, in [3] it was shown that the insertion of PCM inside buildings' envelopes can constitute the solution to overheating problems typical of dry assembled walls and roofs during hot seasons. In the afore mentioned paper the authors applied a multivariate statistical VAR model to approximate the heat exchange performing inside 2003 experimental boxes containing PCM, tested within the framework of an European Commission funded research project entitled "C-Tide" (Changeable Thermal Inertia Dry Enclosures) and demonstrating that the presence of PCM inside the tested walls improved their thermal performances. During the 2004 C-Tide campaign, the experimental setup was sensibly improved, monitoring thermal behavior of PCM containing walls, with the aim of evaluating in a quantitative way the thermal reliefs provided by the use of PCM: it was shown how temperature peaks on internal surface walls are shifted in time and lowered with respect to stratifications without PCM. Moreover, impulse response functions for PCM containing walls are compared with the one without PCM in order to describe and compare their dynamic behaviors: when a unitary shock on temperature of the external layer occurs, these functions show the dynamic reaction of PCM containing walls, while internal temperatures are assumed to be constant.The results reported in this work could be used both by architects, that need to evaluate the opportunity of application of this further stratifications in building envelopes, and by software designers, that must simulate the behavior of PCM containing walls.

This paper is organized as follows: section 2 describes the experimental setup used for the analysis of PCM's performance and data collected; section 3 deals with the time series analysis and it is detailed in other four subsections: the first and the second concerns the theory relative to the statistical models used; in the third 3.3 the model is introduced and estimation outputs are shown; the last subsection 3.4 concerns the development of the statistical model, whose persistence is studied with the impulse response functions as in [3]. Section 4 concludes.

# 2 Experimental setup

As already detailed in previous works [3, 4], tests on cubic experimental boxes measuring 3 m per side are carried out at the Polytechnic University of Marche. The south facing walls of such test buildings, located at the Baraccola area of Ancona, are made up of PCM contained in lightweight envelopes. A test building with a standard dry built lightweight south facing wall without PCM is also used, acting as benchmark. In particular, this paper will analyze data collected during the 2004 experimental campaign, where the two stratifications containing PCM (Box 2 and Box 8) and the one without (Box 6), shown in Fig. 1, were tested and compared with the benchmark.

## 2.1 Experimented prototypes

The stratifications shown in Fig. 1 were installed on the south facing wall of 3 of the 8 experimental boxes built in the "Renewable Energies Outdoor Laboratory", monitoring both temperatures of the walls, internal air and environmental conditions. At present various kinds of PCM are available, each of which having different thermal and physical properties: salt hydrate, polyethylene glycol, fatty acid, paraffin. The PCM used were Glauber salts (a particular type of salt hydrate) with a melting temperature of 32 degrees Celsius, density 1450 $kg/m^3$, latent heat of fusion $1.9 \cdot 10^5\ J/kg$, specific heat in the liquid and solid state equal to $3.6 \cdot 10^3\ J/(kg \cdot K)$, because it has a number of advantages: the ease with which it can be worked at the solid phase (it is available as powder), its fire resistance qualities and its relatively narrow melting range. The walls of Box 2 and 8 were equipped with this kind of PCM, the second stratification having also an air layer external to the PCM one. When external walls are hit by solar radiation, inward flux starts from the exterior towards the interior. The heat flux caused by the external irradiation causes an increase in the temperatures within the wall and increases the gradient over temperature between the exterior and the interior. When the PCM behind the external finish reaches its melting temperature, it absorbs the thermal flux coming from the exterior completely, hence the incoming flux penetrating the internal environment remains low until PCM is completely melted. During the night, thanks to the absence of sunlight and relatively low environmental temperatures, PCM releases all the heat previously absorbed, triggering the solidification process. By the comparison between these two PCM containing walls and the benchmark (Box 6), it is possible to draw conclusions relative to the improvements deriving from the use of this additional layer. In addition, it is possible to evaluate the importance of the insertion of an air layer as well.

Figure 1: South wall stratification of Box 6 (a), Box 8 (b) and Box 2 (c) with sensor positioning: RTDs billed with “R” followed by a number

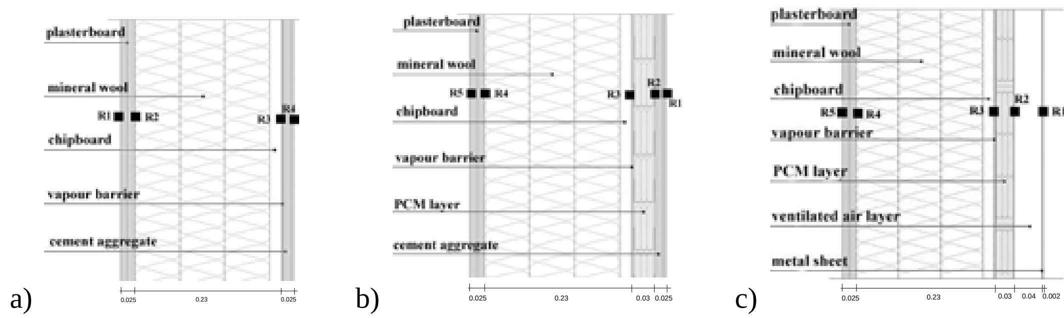


As shown in Fig. 2, in order to reproduce the standard internal environment typical of inhabited buildings, one system for controlling the interior temperatures was installed in each Box, which guaranteed its preservation at a constant value. For this purpose, each Box is divided into two rooms using a plasterboard partition assembled with the interposition of a thermal insulation layer: the technical one containing air at 23.5 degrees Celsius, and the control one with air at 25 degrees Celsius. A control system provided cool air from the technical to the control volume when necessary to maintain constant air temperature in the second room, whose temperature was controlled by “T” type 9 thermocouples. In this way the monitored wall temperature depends on the external environment conditions and on internal fixed air temperature. A datalogger (Datataker DT 500 series 3) with 10 analogical type inputs and 4 digital input-outputs equipped with two channel expansion modules (CEM type) which increase the analogical inputs to 30, 44 for the digital ones and to 10 the relay and digital “open collector” type outputs was installed, to collect data from sensors. All the temperature sensors have 0.1 degrees Celsius sensitivity.

Figure 2: The “Renewable Energies Outdoor Laboratory” (a); Vertical section and plan of the generic Box (b) with sensor positioning (thermocouples of “T” type)

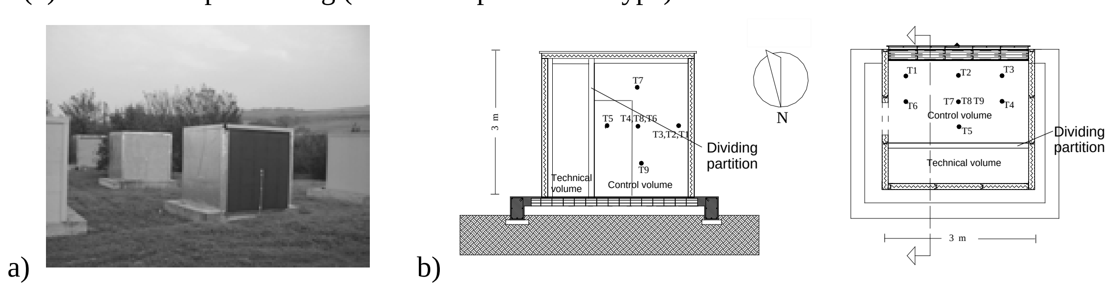


## 2.2 Data

The analysis in section 3.3 is based on the data collected inside the Boxes described in Fig. 2 having the three stratifications shown in Fig. 1. In [4] a wide discussion about the data was presented. Instead, the statistical model is aimed at the approximation of thermal behavior for Box 8, and for Box 2, as compared with the benchmark. Every sensor gives a time series made up of 23904 observations, and there are 27 time series for each of the two boxes with PCM, and 26 series for the one without. Fig. 3 shows the temperature course for sensors R4 in Boxes 2 and 8 and for sensor R3 for Box 6. From such a preliminary analysis, it can be inferred that they are quite similar, therefore a statistical approach is necessary in order to work out quantitative conclusions regarding the difference between them. For the model presented in this contribution, the period contained between 15:55 of 30 July 2004 and 14:40 of 27 August 2004 are selected, for a total amount of 8051 data recorded by the sensors every 5 minutes. To smooth the time series the sample was reduced by computing the mean every three observations: the result is a new sample of 2171 observations for each sensor available, every 15 minutes.

Figure 3: Time series of R4 (Boxes 2 and 8) and R3 (Box 6)

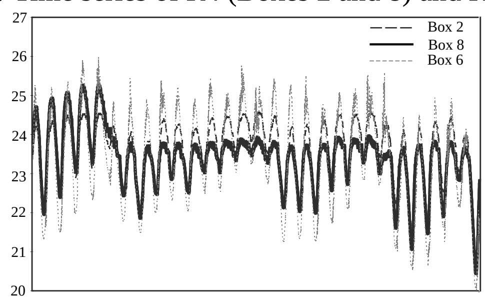


# 3 Empirical analysis

## 3.1 Cointegration and ECM models

Given a vector $X_t$ of $n$ stochastic processes $I(1)$ its components are said to be cointegrated if there is a vector $\beta$ which satisfies the following condition:

$$X_t'\beta \sim I(0) \tag{1}$$

where $I(0)$ and $I(1)$ represent respectively integrated processes of order zero and one[1]. Intuitively it is possible to distinguish two different relationships between all variables in $X_t$: a long run relationship given by the cointegrating vector $\beta$ as shown in equation (1) and a short run one which depends by the deviations of the variables from their long-run trends.

Differencing time series when cointegration exists would not take in account the long run relationship among all variables and so an error correction mechanism (ECM) is required. Given a linear model where dependent variable is cointegrated with regressors, the ECM method simply consists in specifying the model in first difference adding the lagged deviation from equilibrium.

## 3.2 GARCH models

The Auto Regressive Conditional Heteroskedastic (ARCH) class of models, introduced by the seminal paper [7], is based on the intuition that the variance of some variables of interest, conditional on past information may change over time, while the unconditional variance is time invariant. Given a linear model $y_t = x_t'\beta + \varepsilon_t$ such kind of models provides the following specification of the error term:

$$\varepsilon_t = u_t h_t^{1/2} \tag{2}$$

where $u_t \sim N(0,1)$ and $h_t$ is the conditional variance.

This specification is very useful to model the presence of heteroskedasticity and some stylized facts about time series[2]. Many models of time varying conditional variance have been suggested in the literature: the most important innovation is the Generalized ARCH (GARCH) proposed in [9] in which the

[1]A time series is said to be $I(1)$ if its first difference produces a covariance stationary process, while $I(0)$ processes are covariance stationary. See for example [5] or [6] for details.

[2]See [8] for details.

conditional variance obeys the follwing equation:

$$h_t = \omega + A(L)\varepsilon_{t-1}^2 + B(L)h_{t-1} \tag{3}$$

where the number of lags in polynomials $A(L)$ and $B(L)$ gives the GARCH model orders.

Estimation of GARCH models is conducted using the maximum likelihood method[3] and the resulting estimates of unknown parameters are consistent and especially more efficient than OLS.

### 3.3 The model

Given the hypothesis that in the long run the internal wall temperature $y_t$ (sensor R4 for Boxes 2 and 8, sensor R3 for Box 6) satisfies the equation $y_t = \gamma z_t + (1-\gamma)x_t$, where $z_t$ and $x_t$ are respectively T8 and R2 time series, and $0 \leq \gamma \leq 1$ measures the relative importance of the interior for the sensor located on the internal surface of the wall. The first step of the analysis is to estimate the cointegration vector using the dynamic OLS estimator[4] model:

$$y_t - x_t = \gamma(z_t - x_t) + u_t \tag{4}$$

where $u_t$ is an $I(0)$ disturbance, not necessarily white noise. Table 1 shows the estimated parameter $\hat{\gamma}$ for each Box.

Table 1: Dynamic OLS estimation

| **Box** | **Parameter** | **Std. error** |
|---|---|---|
| 2 | 0.946033 | 0.007621 |
| 8 | 0.973427 | 0.010863 |
| 6 | 0.884242 | 0.047149 |

Since $y_t$, $z_t$ and $x_t$ are $I(1)$ processes and the time series $ECM_t = y_t - \gamma z_t - (1-\gamma)x_t \sim I(0)$, the determination of $\gamma$ gives the estimation of the cointegrating vector[5] $\beta = [\ 1 \quad -\hat{\gamma} \quad (\hat{\gamma} - 1\ )]'$; if that vector exists, we need to insert the long run cointegration relationship between the variables into the model and so we select a model in differences with the ECM term. As shown in [3], the OLS method produces residuals affected by a strong presence of heteroskedasticity and, as a consequence, inefficient estimates of the unknown parameters. An IGARCH(1,1) specification is used to solve these problems and, therefore, the model becomes the following[6]:

$$\begin{cases} A(L)\Delta y_t = \mu + B(L)\Delta x_t + C(L)z_t + ECM_{t-1} + \varepsilon_t \\ \varepsilon_t = u_t h_t^{1/2} \\ h_t \sim IGARCH(1,1) \end{cases} \tag{5}$$

where $A(L)$, $B(L)$ and $C(L)$ are polynomials in the lag operator, while $ECM_t$ is the error correction term imposed to evaluate the long run dynamics due to the existence of cointegration. The second and

[3] See [10] for details.

[4] Introduced by Saikkonen(1991) and Stock and Watson (1993), the dynamic OLS method gives superconsistent and asymptotically mixed normal estimates of the unknown parameters. See [11] and [13] for details. The parameters' estimation is carried out using the OLS regression $(y_t - x_t) = a + \gamma(z_t - x_t) + \sum_{i=-m}^{m} b_i \Delta(z_t - x_t) + e_t$, where $m$ is the bandwidth selected. As shown in [14], consistent standard errors are computed via the formula $\hat{se} = \sqrt{\hat{\theta}/\hat{\sigma}^2}$, where $\hat{\sigma}^2$ is the sample variance and the estimate of $\hat{\omega}$ is $(1/T)$ times the sum of the products of $e_t$ with its lagged value with decreasing weights given by the Bartlett method $\hat{\theta} = T^{-1} \sum_{i=-k}^{k} [1 - 1/k] e_t e_{t-i}$

[5] For more details on cointegration see for example [15].

[6] Introduced in [12], Integrated GARCH (IGARCH) models are characterized by the fact that the sum of all coefficient in polynomials in the lag operator are equal to one: this constraint allows to evaluate the situation in which shocks in the conditional variance are persistent in the long run. See [8] for details.

the third expressions in equation (5) refer to the presence of conditional heteroskedasticity in the data set: the former is equation (2) and the conditional variance $h_t$ and the latter gives the specification model for $h_t$, which is

$$h_t = \omega + \alpha\varepsilon^2_{t-1} + (1-\alpha)h_{t-1} \tag{6}$$

Table 2 shows the estimation output of model (5); the number of lags selected in polynomials $A(L)$, $B(L)$ and $C(L)$ are different for each Box, while the GARCH model is always the same[7].

Table 2: Model estimates

| | **Box 2** | | | | **Box 8** | | | | **Box 6** | | | |
|---|---|---|---|---|---|---|---|---|---|---|---|---|
| | Coeff. | Std. Err. | t-Stat | P-value | Coeff. | Std. Err. | t-Stat | P-value | Coeff. | Std. Err. | t-Stat | P-value |
| $\mu$ | -0.0298 | 0.0017 | -17.713 | 0.000 | -0.0626 | 0.0071 | -8.868 | 0.000 | -0.0383 | 0.0026 | -14.659 | 0.000 |
| $\Delta y_{t-1}$ | 0.0938 | 0.0227 | 4.133 | 3.585e-5 | 0.2233 | 0.0242 | 9.236 | 0.000 | 0.0454 | 0.0374 | 1.213 | 0.225 |
| $\Delta y_{t-2}$ | 0.1039 | 0.0207 | 5.029 | 4.929e-7 | -0.0525 | 0.0224 | -2.348 | 0.019 | - | - | - | - |
| $\Delta y_{t-3}$ | 0.0710 | 0.0193 | 3.677 | 0.000 | 0.0325 | 0.0230 | 1.411 | 0.158 | - | - | - | - |
| $\Delta y_{t-4}$ | - | - | - | - | 0.1530 | 0.0227 | 6.743 | 1.554e-11 | - | - | - | - |
| $\Delta y_{t-5}$ | - | - | - | - | 0.0249 | 0.0213 | 1.171 | 0.241 | - | - | - | - |
| $\Delta y_{t-6}$ | - | - | - | - | 0.0465 | 0.0161 | 2.884 | 0.004 | - | - | - | - |
| $\Delta x_t$ | 0.0236 | 0.0048 | 4.867 | 1.132e-6 | -0.0010 | 0.0034 | -0.285 | 0.776 | 0.0740 | 0.0238 | 3.107 | 0.002 |
| $\Delta x_{t-1}$ | -0.0177 | 0.0049 | -3.659 | 0.000 | -0.0049 | 0.0037 | -1.319 | 0.187 | -0.0601 | 0.0263 | -2.284 | 0.022 |
| $\Delta z_t$ | 0.1342 | 0.0057 | 23.656 | 0.000 | 0.1025 | 0.0034 | 30.136 | 0.000 | 0.1396 | 0.0193 | 7.246 | 4.285e-13 |
| $\Delta z_{t-1}$ | 0.0889 | 0.0071 | 12.390 | 0.000 | 0.1389 | 0.0061 | 22.727 | 0.000 | 0.1412 | 0.0264 | 5.343 | 9.122e-8 |
| $\Delta z_{t-2}$ | 0.0341 | 0.0065 | 5.269 | 1.369e-7 | 0.0676 | 0.0063 | 10.681 | 0.000 | 0.0210 | 0.0229 | 0.916 | 0.360 |
| $\Delta z_{t-3}$ | - | - | - | - | 0.0336 | 0.0055 | 6.120 | 9.373e-10 | 0.1134 | 0.0185 | 6.129 | 8.835e-10 |
| $\Delta z_{t-4}$ | - | - | - | - | 0.0165 | 0.0050 | 3.326 | 0.001 | - | - | - | - |
| $\Delta z_{t-5}$ | - | - | - | - | -0.0046 | 0.0044 | -1.052 | 0.293 | - | - | - | - |
| $\Delta z_{t-6}$ | - | - | - | - | -0.0108 | 0.0033 | -3.328 | 0.001 | - | - | - | - |
| $ECM_{t-1}$ | -0.0479 | 0.0028 | -17.026 | 0.000 | -0.0379 | 0.0043 | -8.725 | 0.000 | -0.0272 | 0.0037 | -7.326 | 2.371e-13 |
| $\omega$ | 1.043e-5 | 2.025e-6 | 5.150 | 2.598e-7 | 6.968e-6 | 1.998e-6 | 3.487 | 0.000 | 6.598e-5 | 1.963e-5 | 3.361 | 0.001 |
| $IGARCH$ | 0.2457 | 0.024 | 10.128 | 0.000 | 0.2094 | 0.0394 | 5.314 | 1.076e-7 | 0.3406 | 0.022 | 15.206 | 0.000 |

In Fig. 4 time series of model residuals are plotted together with the time series of $\pm h_t^{1/2}$: the evidence suggests that the IGARCH(1,1) specification provides a good method to fit the the changes in the conditional variance of the data and to model the excess of kurtosis.

Figure 4: Residuals and conditional standard deviation series

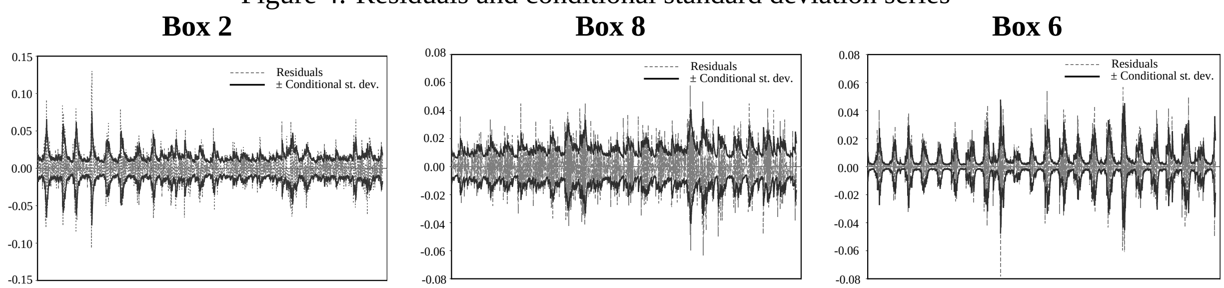


## 3.4 Impulse responses

The impulse response function given by the formula $c_i = \partial y_{t+i}/\partial x_t$ used in [3], is applied to check the reaction of the temperature recorded by the internal sensors $y_t$, given a unitary shock on $x_t$ of the three walls under consideration. In this way it is possible to isolate only the effect of an external temperature increment on the internal surface temperature for each wall by evaluating the differences which exist between their responses. Thus, analyzing the ratio between PCM containing walls and the benchmark one, quantitative indexes of the reduction in the temperature increase given by the presence of PCM are worked out. In Fig. 5 impulse responses of the walls are plotted, where it is clear that the internal temperature increase in the benchmark wall is, at the initial step, much higher than the one monitored by PCM containing walls. The main difference is that when PCM is inserted, walls have a more stable temperature course around their mean temperature, while the benchmark is more sensitive to external

[7] Variable $IGARCH$ refers to $\alpha$ parameter.

conditions. The graphs also show the quantitative relations between them. In comparing walls containing PCM, it is clear that PCM is less useful if there is an air layer on the exterior. For all the walls, after a first initial temperature increase, there is a negative contribution, probably due to the cooling of the dividing partition, that is affected by the system action. In general the south wall of Box 8 is the most stable around its mean temperature, while the one of Box 2 is more sensitive to temperature risings inside its air layer, probably because the presence of flowing air increases the conduction towards PCM even if it is melting (because its conductivity is relatively high and about $0.5\ W/(m \cdot K)$).

From the cumulative courses of the impulse response functions, it is possible to notice that there are strong differences in the long time behavior for the three walls under consideration. In particular, incoming heat flux entering during the whole day inside the benchmark Box without PCM, is able to increase internal temperature much higher and rapidly than the one of Box 2 and 8. Therefore, the first conclusion is that the presence of only one system inside buildings is not able to provide the same comfort conditions, as the internal surface temperature is dependent on the kind of stratification. The second conclusion is that, when the internal environment temperature is maintained at a fixed value, PCM is able to reduce the increment of temperature on the internal surface between about three and six times, depending on the presence of air layers. It can be inferred that the presence of an air layer reduces the importance of PCM, probably because they work in a similar way. Hence, the air layer is really necessary only when the climatic context requires its insertion for the release of the heat flux absorbed during the day by PCM layer, which would not be possible without a ventilated air layer. For climatic contexts like the one where the tests were carried out, an air layer is not necessary.

Figure 5: Impulse responses

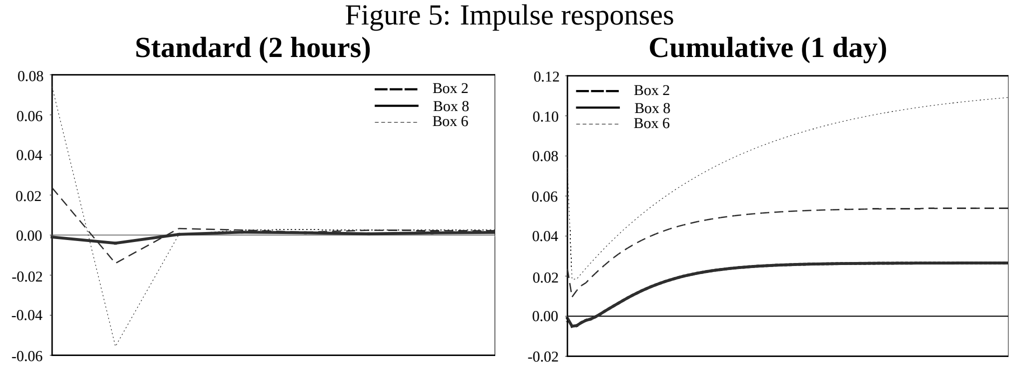


From this analysis it is clear also that PCM containing walls stop their temperature rising before that of the benchmark, and the highest value reached is lower than the reference case. Observing the temperatures delays, it can be noticed that Box 2 is delayed at least half an hour with respect to benchmark one, and never reaches the temperatures of the second. The slope of Box 8 follows the benchmark with a delay of at least two hours, but the temperatures of Box 8 are never equal to the ones of the benchmark.

# 4 Concluding remarks

Using this statistical approach it is possible to approximate the complex functional form that regulates heat transfer inside PCM containing walls, solving the problems given by heteroskedasticity in the previous work [3]. It was useful to provide an approximation of the dynamic behavior of PCM containing walls through the use of impulse response functions, which are referred to a unitary temperature shock on the interface external in respect to the PCM layer and can constitute a valid design tool for architects wanting to infer the behavior of a PCM containing wall, starting from the results of the one without PCM, that can be computed with standard design tools. Moreover, it was demonstrated that the presence of only one system inside buildings is not able to provide comfort conditions, because the internal surface temperature of the benchmark is, in any case, higher than the ones containing PCM.

The small entity of residuals, less than the instruments' sensitivity, demonstrates that the time series model proposed represents a good method to approximate the thermal behavior of PCM containing walls.

## Acknowledgements

We are very grateful to Riccardo "Jack" Lucchetti, professor of Econometrics at the Economics Faculty "G. Fuà", Polytechnic University of Marche, for his helpful comments and suggestions.

## References

[1] Stovall, T. K., Tomlinson, J. J. What are the potential benefits of including latent heat storage in common wallboards?, *Journal of Solar Energy Engineering, Transactions of the ASME*, v 117,n.4, pp. 318-325, (2005).

[2] Neeper, D. A. Thermal dynamics of wallboard with latent heat storage, *Solar Energy*, v 68, n.5, pp. 393-403, (2000).

[3] De Grassi, M., Carbonari, A.;, Palomba, G. A statistical approach for the evaluation of the therml behavior of dry assembled PCM containing walls, *Forthcoming in Building and Environment*, available online *http://authors.elsevier.com/sd/article/S0360132305000740*, (2005).

[4] Principi, P.; Di Perna, C.; Borrelli, G.; Carbonari, A. Experimental energetic evaluation of changeable thermal inertia PCM containing walls, *PALENC 1st International Conference, Santorini, Greece*, 19-21 May, (2005).

[5] Hamilton, J.D. Time series analysis, *Princeton University Press, New Jersey*, (1994).

[6] Greene, W.H. Econometric analysis, *Prentice-Hall*, $3^d$ edition, (1997).

[7] Engle, R.F. Autoregressive conditional heteroskedasticity with estimates of the U.K. inflation, *Econometrica 50*, pp. 987-1008, (1982).

[8] Palm, F.C. GARCH models of volatility, G.S. Maddala & C.R. Rao (eds.), *Handbook of Statistics*, vol. 14, Statistical Methods in Finance, Elsevier, North Holland, (1996).

[9] Bollerslev, T. Generalized autoregressive conditional heteroskedasticity, *Journal of Econometrics* 31, pp. 307-327, (1986).

[10] Bollerslev, T; Engle, R.F.; Nelson, D.B. ARCH models, in R.F. Engle & D.L. McFadden (eds.), *Handbook of Econometrics*, vol. IV, Elsevier, North Holland, (1994).

[11] Saikkonen, P. Asymptotically efficient estimation of cointegrating regressions, *Econometric Theory 7*, pp. 1-21, (1991).

[12] Engle, R.F.; Bollerslev, T. Modelling the persistence of conditional variances, *Econometric Review 5*, pp. 1-50, (1986).

[13] Stock, J.H.; Watson, M. A simple estimator of cointegrating vectors in higher order integrated systems, *Econometrica 61*, pp. 783-820, (1993).

[14] Bartlett, M.S. Periodogram analysis and continuous spectra, *Biometrika 37*, pp. 1-16, (1950).

[15] Johansen S. Estimation and hypothesis testing of cointegration vectors in a Gaussian vector autoregressive models, *Econometrica 59*, pp. 1551-1580, (1991).